

Binding Properties of HABA-Type Azo Derivatives to Avidin and Avidin-Related Protein 4

Susanna Repo,¹ Tiina A. Paldanius,^{2,4}
Vesa P. Hytönen,^{2,5} Thomas K.M. Nyholm,¹
Katrin K. Halling,¹ Juhani Huuskonen,³
Olli T. Pentikäinen,^{1,6} Kari Rissanen,³
J. Peter Slotte,¹ Tomi T. Airene,¹
Tiina A. Salminen,¹ Markku S. Kulomaa,^{2,4}
and Mark S. Johnson^{1,*}

¹Department of Biochemistry and Pharmacy
Åbo Akademi University

Tykistökatu 6
FI-20520 Turku

Finland

²NanoScience Center

Department of Biological and Environmental Science

³NanoScience Center

Department of Chemistry

P.O. Box 35

FI-40014 University of Jyväskylä

Finland

Summary

The chicken genome encodes several biotin-binding proteins, including avidin and avidin-related protein 4 (AVR4). In addition to *D*-biotin, avidin binds an azo dye compound, 4-hydroxyazobenzene-2-carboxylic acid (HABA), but the HABA-binding properties of AVR4 are not yet known. Differential scanning calorimetry, UV/visible spectroscopy, and molecular modeling were used to analyze the binding of 15 azo molecules to avidin and AVR4. Significant differences are seen in azo compound preferences for the two proteins, emphasizing the importance of the loop between strands β 3 and β 4 for azo ligand recognition; information on these loops is provided by the high-resolution (1.5 Å) X-ray structure for avidin reported here. These results may be valuable in designing improved tools for avidin-based life science and nanobiotechnology applications.

Introduction

Avidin, a basic glycoprotein from egg white, and streptavidin, the bacterial relative of avidin, bind a small vitamin molecule, *D*-biotin, with extremely high affinity ($K_D = 10^{-13}$ to 10^{-15} M) [1, 2]. The nature of the specific, strong protein-ligand interaction has been extensively studied in order to identify the structural determinants of the high-affinity binding [3–5] and to engineer novel features in the development of more sophisticated tools for biotechnology applications [6–8]. Although the three-

dimensional (3D) structures of both avidin and streptavidin in complex with *D*-biotin have been solved [9, 10], understanding the details of the biotin-binding process remains challenging [11].

Avidin belongs to a gene family that contains several avidin-related genes (AVRs) [12, 13] whose biological function is unknown. Previously, we produced AVRs in recombinant forms in both *E. coli* [14] and insect cells by utilizing a baculovirus expression system [15, 16]. AVRs possess fascinating properties: despite their lower biotin-binding affinity compared with avidin [15, 16], some AVRs have higher thermal stability than avidin [16, 17]. The 3D structures of AVR2 [17] and AVR4 [18] have been solved to high resolution.

Avidin has a moderate level of affinity for a small molecule, an azo dye called HABA (4-hydroxyazobenzene-2-carboxylic acid, also called 2-(4'-hydroxybenzene) azobenzoic acid; see the structure in Table 1) [19]. Avidin-HABA binding is accompanied by a change in the spectral properties of the dye from yellow to red, a property used to measure the number of biotin-binding sites of avidin derivatives; the reaction is easily reversed by *D*-biotin. The spectroscopic features of HABA in avidin-based applications would obviate the need for radioactive labels; however, because the dissociation constant of the avidin-HABA interaction is only 6×10^{-6} M [19], HABA derivatives with higher affinity for avidin are needed for improved sensitivity. The 3D structure of the avidin-HABA complex has been solved: HABA binds to avidin as a hydrazone tautomer, planarity is thus lost, and an intramolecular hydrogen bond is formed [20]. Streptavidin also binds HABA as the hydrazone tautomer [21], although the affinity is lower (1×10^{-4} M) than that of avidin [2]. The 3D structure of the streptavidin-HABA complex has been solved [21].

Biotin binding to (strept)avidin leads to changes in the conformation [9, 10], stability [22], and rigidity [23] of the proteins. The most flexible part of avidin that interacts with biotin is a loop located between β strands 3 and 4 (L3,4 loop). In the X-ray structure of apo-avidin, the L3,4 loop is disordered [24]. The electron density maps of the avidin-biotin complex structure are clearly interpretable, and the L3,4 loop has a defined conformation [10]. Similarly for streptavidin, the corresponding loop is disordered in the absence of ligand [25]. Two states of the L3,4 loop, "open" and "closed," that are partially determined by the properties of the bound ligand have been observed in streptavidin [25]. In AVR4, the L3,4 loop adopts nearly identical conformations with and without bound biotin [18]. The L3,4 loop is disordered in the avidin-HABA structure [20], while the L3,4 loop adopts the "closed" conformation in structures of streptavidin complexed with HABA and HABA derivatives [21, 26].

We have used various techniques to improve our understanding of the binding process of azo compounds to avidin and AVR4. We synthesized a set of 15 azo compounds (see [Experimental Procedures](#) and [Supplemental Data](#) [available with this article online]) and studied their interactions with the biotin-binding proteins by using differential scanning calorimetry

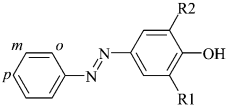
*Correspondence: johnson4@abo.fi

⁴Present address: Institute of Medical Technology, FI-33014 University of Tampere, Finland.

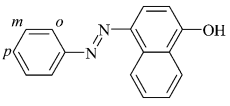
⁵Present address: Department of Materials, ETH Zurich, CH-8093 Zürich, Switzerland.

⁶Present address: Department of Biological and Environmental Science, P.O. Box 35, FI-40014 University of Jyväskylä, Finland.

Table 1. Functional Groups of the Synthesized Ligands



Compound	-COO ⁻ Position	R1	R2
HABA	<i>ortho</i>	H	H
1b	<i>meta</i>	H	H
1c	<i>para</i>	H	H
2b	<i>meta</i>	H	NO ₂
2c	<i>para</i>	H	NO ₂
4a	<i>ortho</i>	CH ₃	CH ₃
4b	<i>meta</i>	CH ₃	CH ₃
4c	<i>para</i>	CH ₃	CH ₃
5a	<i>ortho</i>	H	OH
5b	<i>meta</i>	H	OH
5c	<i>para</i>	H	OH
6b	<i>meta</i>	OH	CH ₃
6c	<i>para</i>	OH	CH ₃



Compound	-COO ⁻ Position
3a	<i>ortho</i>
3b	<i>meta</i>
3c	<i>para</i>

(DSC), UV/visible spectroscopy, and molecular modeling. Moreover, to our knowledge, we present the first high (1.48 Å)-resolution X-ray structure of chicken avidin.

Results

High-Resolution Crystal Structure of Avidin

To our knowledge, we report the first high-resolution X-ray structure of avidin at 1.48 Å resolution. The structure-determination statistics are in Table 2. The fold of the two monomers in the asymmetric unit and tetrameric assembly are nearly identical to the known avidin structures [20, 24, 27–31]: eight antiparallel β strands form a classic β barrel, with one open end serving as the biotin-binding site.

In contrast to other avidin structures, both the open and closed conformations of the L3,4 loop are observed in the electron density maps of this high-resolution structure (Figure 1A). In the closed conformation, the 12 residue-long L3,4 loop seals the ligand-binding pocket similarly to one of the avidin-biotin complexes (PDB code 1AVD [31]). In the 1.48 Å resolution structure, all residues within the L3,4 loop of the closed conformation could be traced in the electron density maps. The open conformation of the L3,4 loop diverges from the closed loop conformation at I34 and reunites with the closed loop conformation at K45. V37–S41 of the open loop conformation could not be traced through the electron density map. Thus, T35–A36, at the start of the L3,4 loop, and N42–K45, at the loop's end, could be built into the electron density of the open loop conformation (Figure 2A).

Before data collection, an avidin crystal was soaked with compound 3a. Despite the color change observed

Table 2. Structure Determination Statistics for Avidin

Data Collection ^a	
Wavelength (Å)	0.804
Beamline	X13
Detector	CCD
Resolution (Å)	20–1.48 (1.58–1.48)
Unique observations	41,811 (7320)
I/σ	10.4 (2.9)
R factor ^b (%)	7.3 (47.0)
Completeness	99.3 (99.1)
Redundancy	4.0 (4.1)
Refinement	
Space group	P2 ₁ 2 ₁ 2
Unit cell	
a, b, c (Å)	72.9, 78.8, 43.0
α, β, γ (°)	90, 90, 90
Monomers per asymmetric unit	2
Resolution (Å)	20–1.48
R _{work} (%)	16.5
R _{free} (%)	19.0
Protein atoms	2,066
Heterogen atoms	36
Solvent atoms	149
Rmsd	
Bond lengths (Å)	0.013
Bond angles (°)	1.5
Ramachandran plot	
Residues in most favored regions	92.5%
Residues in additional allowed regions	7.5%

The PDB code for avidin is 1VYO.

^aThe numbers in parentheses refer to the highest-resolution bin.

^b Observed R factor was taken from XDS [38].

after the soaking experiment, compound 3a was not observed in the solved structure, but, instead, two glycerol molecules are in the ligand-binding pocket. The lack of detection of compound 3a in the binding pocket may be explained by the low occupancy of the ligand in the binding sites. Thus, the ligand might be “invisible” in the crystal structure even though it might have bound to some protein molecules in the soaking experiment.

DSC Analysis

The effect of the azo compounds on the stability of avidin and AVR4 was studied by using DSC (Table 3). Since increases in protein thermal stability upon ligand binding depends on the binding affinity, we have calculated the apparent binding constants at the temperature of protein unfolding, $K_b(T_m)$. Calculations are based on the temperature of protein unfolding in the absence and presence of ligand as well as on the change in enthalpy and heat capacity upon unfolding of the protein in the absence of ligand [32]. HABA, $K_D = 7 \times 10^{-6}$ M at pH 7 at room temperature [33], and 2,6-ANS, $K_D = 2 \times 10^{-4}$ M [34], which have moderate binding affinity for chicken avidin, were used as the control ligands. We also measured the stabilizing effect of the extreme affinity ligand, *D*-biotin, for avidin ($K_D \approx 10^{-15}$ M) and AVR4 ($K_D \approx 10^{-14}$ M) [1, 16].

Of the 18 ligand molecules that were analyzed, biotin produced the largest increase in avidin stability, $\Delta T_m = 34.5^\circ\text{C}$ with $K_b(T_m)$ (M^{-1}) = 3.1×10^{11} , and in AVR4 increased stability $\Delta T_m = 17.2^\circ\text{C}$ with $K_b(T_m)$

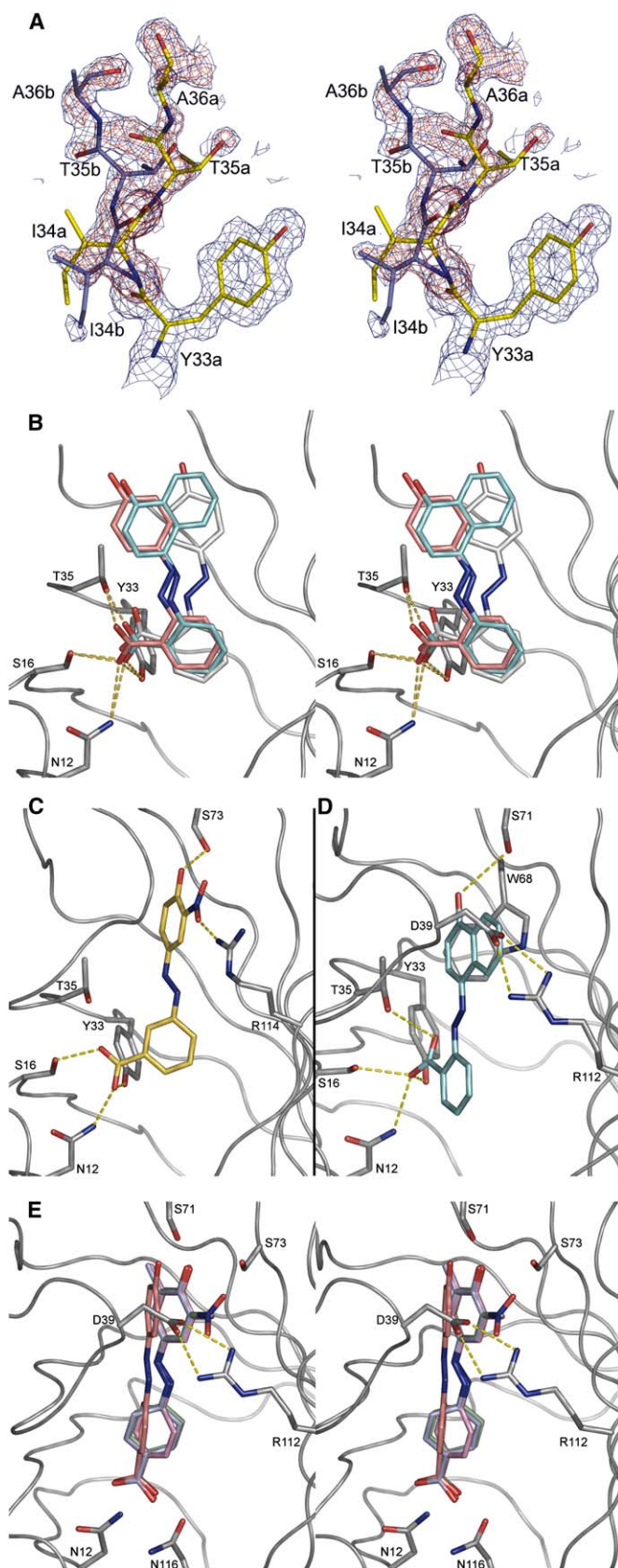


Figure 1. The L3,4 Loop and the Suggested Binding Mode of Some Azo Compounds

(A) The weighted $2F_o - F_c$ (blue) and $F_o - F_c$ (red) electron density maps of avidin showing the branch site for the two alternative L3,4 loops. The maps were calculated in the absence of the amino acids of the L3,4 loop (residues 34–45) and are shown here (a 2.2 Å radius around the atoms) along with the residues Y33, I34, T35, and A36 of the final structure of avidin (PDB code 1VYO). Contours are shown at 1.0σ and 3.0σ for the $2F_o - F_c$ and $F_o - F_c$ maps, respectively. Carbon atoms of residues from the “closed” (a) and “open” (b) conformation of the L3,4 loop are colored yellow and blue, respectively.

(B–E) The secondary structure of the protein in question is shown as a gray coil. Amino acids are represented as sticks; carbon atoms are shown in gray, oxygen atoms are shown in red, and nitrogen atoms are shown in blue. Putative hydrogen bonds are shown as dashed, yellow lines. (B) The suggested binding mode of HABA (orange) and 3a (cyan) to avidin with the open L3,4 loop conformation. HABA (with light-gray carbon atoms) was also docked into the closed loop conformation of avidin. (C) The suggested binding mode of 2b (yellow) to avidin. (D) The suggested binding mode of 3a (cyan) to AVR4. (E) The suggested binding mode of 1c (orange), 2c (green), 4c (purple), and 6c (pink) to AVR4. For details on the suggested binding modes, see the main text.

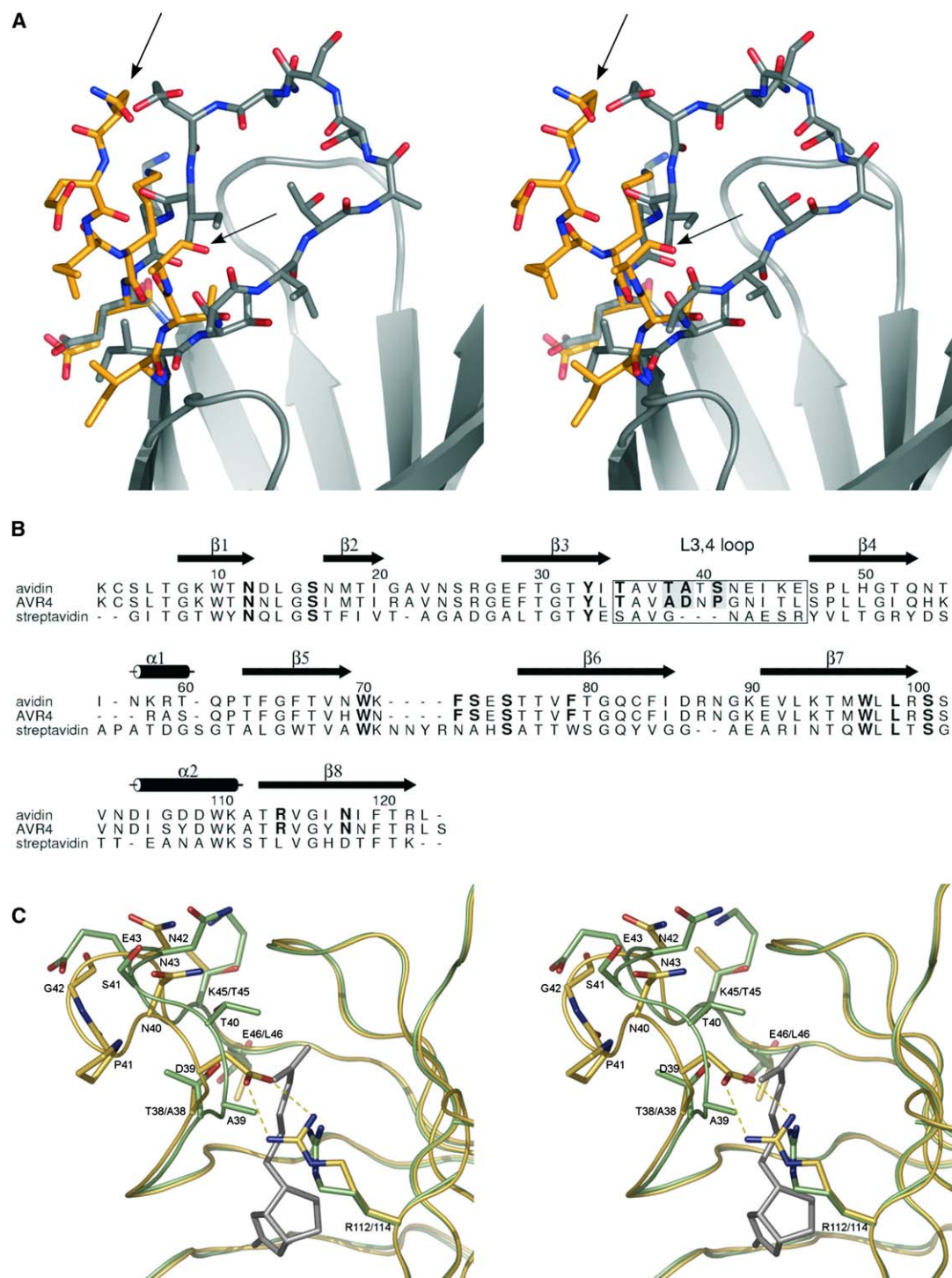


Figure 2. Two Conformations of the L3,4 Loop in Avidin, Structure-Based Sequence Alignment, and Comparison of the L3,4 Loop in Avidin and AVR4

(A) The high-resolution crystal structure of avidin (PDB code 1VYO). The secondary structure is shown in gray, and the amino acids in the L3,4 loop (134–E46) are shown as sticks. The closed L3,4 loop conformation is in gray, and the open conformation is in orange. The arrows indicate the ends of the peptide chain in the open loop conformation.

(B) The structure-based sequence alignment of avidin (PDB code 1VYO), AVR4 (PDB code 1Y55), and streptavidin (PDB code 1SWE). The secondary structure elements of avidin are indicated, and the L3,4 loop of avidin, AVR4, and streptavidin is boxed. The key residues for azo compound binding in avidin and AVR4 are in bold (and when conserved, they are also in bold for streptavidin). The shaded residues indicate the most important differences (for details, see the text) between avidin and AVR4 sequences in the L3,4 loop. The alignment was performed with Vertaa implemented in Bodil [51], and the picture was produced with Alscript [54].

(C) The L3,4 loop of avidin (PDB code 1VYO, green) and of AVR4 (PDB code 1Y55, yellow). The structures were superimposed with Vertaa in Bodil [51]. Biotin, docked into the 1VYO structure with GOLD 2.2 [49], is shown in gray. Amino acids of the L3,4 loop, together with a conserved arginine residue from β8, are labeled and shown as sticks.

Table 3. The Transition Melting Temperature, T_m , of Avidin and AVR4 Determined in the Presence of Different Ligands

Ligand	Avidin			AVR4		
	T_m (°C)	ΔT_m (°C)	$K_b(T_m)^a$ (M^{-1})	T_m (°C)	ΔT_m (°C)	$K_b(T_m)$ (M^{-1})
—	82.5	—	ND ^b	109.9	—	ND ^b
HABA	92.8	10.3	2.9×10^5	110.9	1.0	3.2×10^3
1b	91.3	8.8	1.8×10^5	110.9	1.0	3.2×10^3
1c	86.3	3.8	2.0×10^4	114.9	5.0	4.2×10^4
2b	95.3	12.8	1.0×10^6	113.9	4.0	2.6×10^4
2c	87.1	4.6	2.6×10^4	115.6	5.7	5.8×10^4
3a	98.4	15.9	5.0×10^6	116.9	7.0	1.0×10^5
3b	91.5	9.0	1.8×10^5	111.1	1.2	4.0×10^3
3c	93.0	10.5	3.6×10^5	113.0	3.1	1.6×10^4
4a	95.6	13.1	1.2×10^6	113.6	3.7	2.2×10^4
4b	87.9	5.4	3.8×10^4	109.8	-0.1	ND ^b
4c	84.3	1.8	5.4×10^3	114.9	5.0	4.2×10^4
5a	94.5	12.0	7.0×10^5	112.2	2.3	9.8×10^3
5b	90.4	7.9	1.1×10^5	112.1	2.2	9.2×10^3
5c	86.5	4.0	2.0×10^4	114.5	4.6	3.5×10^4
6b	86.5	4.0	2.1×10^4	111.5	1.6	5.9×10^3
6c	84.1	1.6	4.9×10^3	115.2	5.3	4.8×10^4
2,6-ANS	84.6	2.1	6.8×10^3	114.8	4.9	4.0×10^4
D-biotin	117.0 ^c	34.5	3.1×10^{11}	127.1	17.2	1.3×10^7

^a The apparent binding constant (K_b) is calculated from data obtained at the T_m as described in Brandts et al. [32].

^b Not determinable.

^c From Hytönen et al. [16].

(M^{-1}) = 1.3×10^7 . HABA significantly increased avidin stability ($\Delta T_m = 10.3^\circ\text{C}$, and $K_b[T_m]$ [M^{-1}] = 2.9×10^5), as did the five other azo compounds ($\Delta T_m > +10.0^\circ\text{C}$). Three molecules are *ortho*-derivatives of HABA (3a, 4a, and 5a), one is a *meta*-derivative (2b), and one is a *para*-derivative (3c). Overall, the stabilizing effect of the *ortho*-derivatives of HABA was largest: on average, $\Delta T_m = 12.8^\circ\text{C}$ and $K_b(T_m)$ (M^{-1}) = 1.8×10^6 . The *meta*-derivatives showed somewhat poorer stabilization of avidin (average $\Delta T_m = 8.0^\circ\text{C}$; $K_b[T_m]$ [M^{-1}] = 2.5×10^5), while the *para*-derivatives were the least effective in terms of stabilizing the avidin complex (average $\Delta T_m = 4.4^\circ\text{C}$; $K_b[T_m]$ [M^{-1}] = 7.3×10^4). The control ligand, 2,6-ANS, stabilized avidin rather poorly, with $\Delta T_m = 2.1^\circ\text{C}$ and $K_b(T_m)$ (M^{-1}) = 6.8×10^3 .

In comparison to avidin, AVR4 showed somewhat different behavior in the presence of the azo compounds. HABA was relatively inefficient in stabilizing AVR4 ($\Delta T_m = 1.0^\circ\text{C}$ and $K_b[T_m]$ [M^{-1}] = 3.2×10^3), as were the other *ortho*-derivatives (average $\Delta T_m = 3.5^\circ\text{C}$; $K_b[T_m]$ [M^{-1}] = 3.4×10^4), in contrast to the *para*-derivatives with, on average, a ΔT_m of 4.8°C and $K_b(T_m)$ (M^{-1}) = 4.0×10^4 . The *meta*-derivatives were the least effective in stabilizing AVR4: with, on average, a $\Delta T_m = 1.7^\circ\text{C}$ and $K_b(T_m)$ (M^{-1}) = 9.7×10^3 . Interestingly, 2,6-ANS stabilized AVR4 with a $\Delta T_m = 4.9^\circ\text{C}$ and $K_b(T_m)$ (M^{-1}) = 4.0×10^4 , similar to the average values for the *para*-derivatives.

Altogether, the DSC analyses suggest that avidin and AVR4 do not have similar binding affinities for the azo compounds. Avidin exhibits stronger binding for the *ortho*-forms, whereas AVR4 binds the *para*-forms more strongly. Furthermore, AVR4-2,6-ANS binding appears to be stronger than that of avidin.

UV/Visible Spectroscopy

The spectral characteristics of the azo compounds in aqueous solution were characterized by UV/visible

spectroscopy. Between 300 and 650 nm, two peaks were found at 350.7 nm and 457.9 nm (average values) in the absorption spectrum for most compounds. Avidin is known to affect the absorption spectrum of HABA dramatically [33]. Consequently, we examined the spectral properties of HABA derivatives in the presence of avidin and AVR4. In general, changes in the absorbance spectrum reflect alterations in the physicochemical environment surrounding the ligand in the protein-bound form as well as any changes in double bond conjugation that result from binding. We mainly observed bathochromic shifts of the absorption maximum; however, in some instances, hypsochromic shifts of the absorption maximum were also observed. In the case of HABA, there are two peaks, at 346 nm and 439 nm in the absorbance spectrum. These peaks are due to the two tautomeric conformations of HABA; upon binding avidin, the conformation absorbing near 500 nm is favored. It has been shown that HABA bound to avidin forms the hydrazone tautomer [20]. Thus, there are two simultaneous changes that result from interactions with azo ligands: (1) the accumulation of a specific ligand conformation, which leads to absorption intensity differences between peaks; and (2) spectral shifts that are the result of inter- and intramolecular hydrogen bond formation and rearrangement of double bonds. Here, the spectral shifts are most informative, since they provide information on the relative strength of the avidin and AVR4 complexes with the azo compounds. The measured absorbance peak maxima (A_{max}) are listed in Table 4.

Similarly to HABA, the presence of avidin caused the longer-wavelength peak of the *ortho*-derivatives to move toward longer wavelengths (the average $\Delta A_{\text{max}} = 34$ nm). This increase in the maximum absorption wavelength probably results from the formation of an intramolecular hydrogen bond in the *ortho*-derivatives of the azo compounds [33]. Such radical changes were not seen in the absorbance spectra of the *meta*- and

Table 4. Spectral Analysis of the Azo Molecules in the Absence and Presence of Avidin and AVR4

Ligand	$A_{\max}(1)^a$	$A_{\max}(2)$	+Avidin		+AVR4	
			$A_{\max}(1)$	$A_{\max}(2)$	$A_{\max}(1)$	$A_{\max}(2)$
HABA	346	439	343	496	339	494
1b	348	431	343	432	332	413
1c	354	438	357	441	393	ND ^b
2b	371	419	364	431	351	422
2c	378	430	389	456	382	452
3a	325	493	329	522	335	518
3b	324	482	331 ^c	499	330 ^d	488
3c	327	481	340	511	357	519
4a	350	477	323	500	325	497
4b	354	444	349	444	343	447
4c	360	456	360	457	358	469
5a	360	474	ND ^e	501	ND ^e	499
5b	359	454	375	442	363	453
5c	367	461	362	470	ND ^b	479
6b	343	472	340	477	318	446
6c	347	474	347	474	343	470

^a The measured spectra of the azo molecules was analyzed by fitting two Gaussian peaks to the data, and the absorption maxima (in nm) were determined from the fitted curves.

^b Only one peak was observed in the spectrum.

^c A new peak with A_{\max} at 405 nm also appeared.

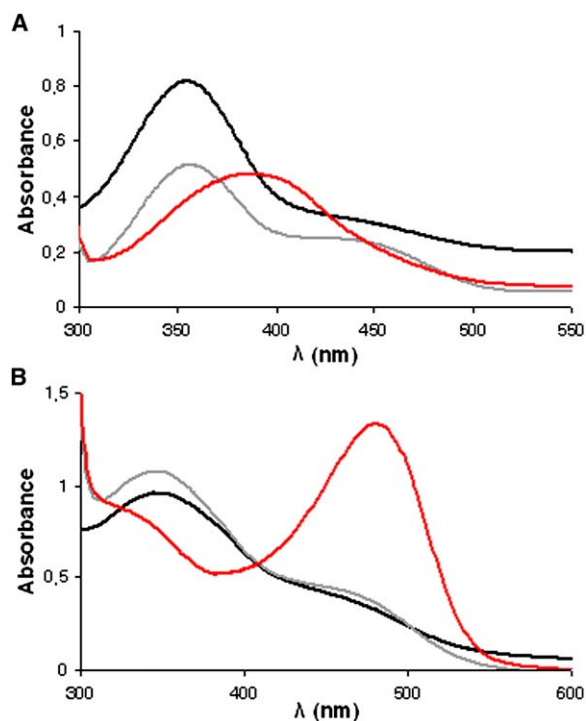
^d A new peak with A_{\max} at 411 nm also appeared.

^e The lower-wavelength peak was negligible.

the *para*-forms (average $\Delta A_{\max} = 3.8$ nm and 11.5 nm, respectively). Compounds **3a**, **3c**, **4a**, and **5a** with avidin result in the largest spectral changes, suggesting that the compounds have high affinity for avidin, while compounds **1c**, **3b**, and **5c** led to moderate spectral changes. Compounds **1b**, **4b**, **4c**, and **5b** with avidin produced only negligible changes in the spectra. The spectroscopic data for compounds **2b** and **2c** is unclear, and the affinity of these compounds for avidin cannot be inferred from the data.

Like avidin, the presence of AVR4 induced similar spectral changes in the maximum peak found at longer wavelengths for the *ortho*-compounds (average $\Delta A_{\max} = 31.3$ nm). For the *meta*-forms, AVR4 induced a slight decrease in A_{\max} at longer wavelengths (average $\Delta A_{\max} = -5.5$ nm), while the A_{\max} of the *para*-forms increased by 14.5 nm in the presence of AVR4. According to the spectroscopic studies, compounds **1c**, **3a**, **4a**, **5a**, and **5c** seem to produce the most significant spectral changes, which is indicative of high affinity for AVR4, while HABA and compound **3b** lead to moderate spectral changes; compounds **1b**, **2c**, **3c**, **4b**, **4c**, **5b**, **6b**, and **6c** produced only negligible changes to spectra in the presence of AVR4, suggesting that AVR4 has a low binding affinity for each compound.

In this analysis, the most interesting difference between avidin and AVR4 was found with compounds **1c** and **5c** (Figure 3). In the presence of avidin, the spectral changes of these compounds were negligible. The presence of AVR4, however, introduced a single peak centered at 393 nm in the case of **1c** (Figure 3A) and at 479 nm in the case of **5c** (Figure 3B). The induction of a single peak upon protein-ligand interaction suggests that a single tautomer of both **1c** and **5c** binds to AVR4 with higher affinity than for the corresponding avidin complexes. Based on the available data, however, we

Figure 3. UV/Visible Spectra of **1c** and **5c**

(A) The UV/visible spectra of 4-hydroxyazobenzene-4-carboxylic acid (**1c**; black) with avidin (gray) and AVR4 (containing the mutation C122S; red).

(B) The UV/visible spectra of 3',4-dihydroxyazobenzene-4-carboxylic acid (**5c**; black) in the presence of avidin (gray) and AVR4 (C122S; red).

are not able to determine which tautomer of **1c** and **5c** is in question. Heavy computational calculations or high-resolution crystal structures would be needed to answer that question. With **3b**, a unique peak with an A_{\max} of ~ 410 nm appeared with both avidin and AVR4. This peak emerges at a wavelength between the shorter (~ 300 nm)- and the longer (~ 500 nm)-wavelength peaks seen for **3b** and the other azo compounds. This is an interesting observation requiring further study. Overall, compared with avidin, AVR4 induced larger changes in the spectra of the *para*-derivatives of the azo compounds (average $\Delta A_{\max} = 11.5$ nm for avidin and 14.5 nm for AVR4).

Ligand Docking Studies

All 15 azo compounds that were synthesized (Table 1), as well as HABA and 2,6-ANS, were docked into 3 different structures: the avidin structure (PDB code 1VYO) in both the closed and open conformations and the AVR4 structure (PDB code 1Y55). The sequences of avidin and AVR4 are 77% identical [18], and the major differences that could affect ligand binding are located along the L3,4 loop (residues 35–46). The sequence alignment between avidin and AVR4 is shown in Figure 2B. The L3,4 loop in avidin and AVR4 is 12 amino acids long, but there are several large differences in the properties of residues forming the loop in each protein: a salt bridge is formed in AVR4 between D39 (A39 in avidin)

and R112 (R114 in avidin, see Figure 2C), and a proline residue at position 41 is S41 in avidin.

Altogether, the experimental studies identified five azo compounds with affinities for avidin that are similar to (3c) or larger (2b, 3a, 4a, and 5a) than the affinity of HABA for avidin. According to the docking studies, the benzoate group of the three best *ortho*-compounds, 3a, 4a, and 5a, would form interactions identical to those observed in the avidin-HABA complex structure [20]. An oxygen atom in the benzoate group of 3a, 4a, and 5a is positioned so that it could hydrogen bond with S16 and T35 (unless specified otherwise, interactions are with the side chain of the indicated residue), while a second oxygen atom would form up to three hydrogen bonds with N12, S16, and Y33 (Figure 1B). In addition, the benzoate ring would interact with F79, W97, and W110 from the adjoining monomer. The docking studies indicate that the additional phenyl ring of 3a fully occupies a pocket formed by W70, F72, S73, S75, and L99. Similarly, one of the methyl groups found in 4a and the additional hydroxyl group of 5a are also docked into this pocket (the hydroxyl group hydrogen bonding with S73), but the methyl and the hydroxyl groups on their own are not bulky enough to fill the pocket.

Compound 2b is a *meta*-derivative of HABA and has an additional NO₂ group. As docked, the *meta*-carboxylate group would be buried deeper within the binding pocket of avidin compared to the *ortho*-derivative. According to the docking results, it appears likely that there is a hydrogen bond between one of the carboxylate oxygens of the ligand and S16, as well as two hydrogen bonds between the other carboxylate oxygen and N12 and Y33 (Figure 1C). Upon avidin binding, the NO₂ group of 2b is most likely accommodated at a solvent-accessible site next to S75, S101, and R114, where the NO₂ group would be positioned to form hydrogen bonds with R114.

The *para*-compound 3c has a similar affinity to avidin as HABA. The interactions of 3c, at the bottom of the ligand-binding pocket, include possible hydrogen bonds with N12 and N118 and hydrophobic interactions with F79, W97, and W110 from the adjoining monomer. 3c is longer than the *ortho*-compound 3a; as a consequence, 3c would extend further out of the binding pocket.

Experimental results show that 2,6-ANS binds to AVR4 with a significantly higher affinity than to avidin, in good agreement with our docking studies that showed that 2,6-ANS fits nicely into the binding pocket of AVR4 and that the phenyl ring of 2,6-ANS would stack with W68 and F70. In addition, the interaction of the SO₃ group of 2,6-ANS with AVR4 appears more favorable than with avidin: the SO₃ group could hydrogen bond to N12, S16, Y33, and N116 of AVR4. When docked to avidin, the phenyl ring of 2,6-ANS would clash with residues of the L3,4 loop, especially with T40.

Interestingly, the experimental studies indicate that all but two of the HABA derivatives (1b and 4b) have affinities for AVR4 that are higher than the affinity of HABA for AVR4. The docking studies indicate that regardless of the closed conformation of the L3,4 loop of AVR4, the azo compound with the highest affinity for AVR4 (and for avidin), 3a, can fit into the binding pocket of AVR4. The naphthalene group of 3a is capable of forming π - π

stacking interactions with W68. In addition, a hydrogen bond could form between S71 (Figure 1D) and the hydroxyl group of 3a. Interactions with the benzoate group of 3a in the docked complexes are identical to those observed for the avidin-HABA complex [20].

The *para*-derivatives of HABA, 1c, 2c, 4c, 5c, and 6c, have very similar affinity for AVR4, and according to the docking studies, the binding mode of these compounds to AVR4 is also similar to each other. The benzoate group of the *para*-compounds is positioned where it could form hydrogen bonds with N12 and N116, at the bottom of the ligand-binding pocket of AVR4 (Figure 1E), as well as hydrophobic interactions with Y33, F77, W95, and W108 from the adjacent monomer. In addition, the phenolic part of the compounds is nicely docked between the hydrophobic side chains of A38, W68, F70, and L97, and a hydrogen bond can be positioned to link the phenolic hydroxyl group and the hydroxyl group of S71. The *para*-compound with the highest affinity for AVR4, 2c, has an NO₂ group attached to the phenol ring. The docking studies show that this polar group could hydrogen bond with S73 and R112 (Figure 1E). The additional hydroxyl group of 6c seems capable of hydrogen bonding with D39 and S73, while the additional methyl group is docked between the side chains of W68 and F70. Compounds 1c and 4c show equal affinity for AVR4. 1c more closely resembles HABA in that no additional groups are attached to the phenol ring, whereas 4c has two additional methyl groups on the ring. One of the methyl groups is docked between the side chains of W68 and F70, and the other methyl group is accommodated within a region formed by D39, S73, L97, and R112.

Discussion

In egg white, biotin binding is virtually irreversible and is needed to protect the growing embryo from infection by microbes. For applications in biotechnology, however, such irreversible binding is not always useful. While there is no need, and it is probably not even possible, to design any ligands with affinity better than that of *D*-biotin, research has focused on finding compounds with high, but reversible, affinity for avidin. The organic dye compound HABA (4-hydroxyazobenzene-2-carboxylic acid), with moderate affinity for avidin, is a good starting point for the design of novel avidin-binding compounds. Due to the spectroscopic features of HABA and its derivatives, their use in avidin-based applications would be safer than assays employing radioactive labels.

The formation of the complex between HABA and avidin is accompanied with a change in the spectral properties of HABA [33]. In the original paper, Green also reported that a *meta*-derivative of HABA bound to the avidin biotin-binding site, although the spectral changes were less dramatic. Similar spectral changes were observed for the complex of HABA and streptavidin, but the affinity of HABA for streptavidin ($K_D = 100 \times 10^{-6}$ M) is less than for avidin ($K_D = 6 \times 10^{-6}$ M) [19, 33]. Green has also reported the specific binding of other similar dye compounds to the biotin-binding site of avidin [33]. Much later, Weber et al. [26] successfully developed derivatives of HABA that show higher affinity toward streptavidin.

Avidin has been reported to have pseudocatalytic activity, meaning that avidin is capable of enhancing the hydrolysis of biotinyl ester derivatives, whereas streptavidin efficiently protects the same derivatives from hydrolysis [27]. This and other studies on the pseudocatalytic activity of avidin and streptavidin demonstrate the importance of the L3,4 loop as a molecular regulator in constraining the binding of biotin and biotin derivatives and in converting the protein into a pseudoenzyme [18, 35]. Comparisons of the crystal structures of streptavidin have shown that the L3,4 loop can adopt two structural states depending on the bound ligand [25]. In the case of avidin, the corresponding loop is disordered in the apo form [24], but biotin binding stabilizes the conformation of the loop and “locks” it into the closed state [10].

According to the experimental studies presented here, the *ortho*-derivatives of HABA bind better to avidin, whereas the *para*-derivatives bind better to AVR4. The avidin and AVR4 sequences are very similar throughout the secondary structure elements, except for the L3,4 loop (Figure 2B). Based on the docking studies, we suggest that the *ortho*-derivatives of HABA bind avidin with a conformation of the L3,4 loop that is more open. The results previously reported by Ellison et al. [36] also support this hypothesis. They have shown that HABA increases the affinity of proteinase K for avidin, and that, as a result, the L3,4 loop of avidin is cleaved. Furthermore, in the crystal structure of the avidin-HABA complex the L3,4 loop is not visible [20], suggesting that it is mobile. According to the docking results, if the benzoate group of HABA is docked into the closed loop conformation of avidin, it is not able to maintain hydrogen-bonding interactions with residues (N12, S16, T35, and Y33) along the “bottom” of the binding pocket (Figure 1B). Taken together, the current experimental data and docking studies support a model for HABA binding to avidin in which HABA increases the mobility of the L3,4 loop.

In the AVR4 structure, the conformation and flexibility of the L3,4 loop is constrained by the salt bridge formed between the side chains of D39 and R112 [18]. In contrast, the L3,4 loop of avidin is not constrained by a salt bridge, resulting in more conformational flexibility. Consequently, the *ortho*-compounds cannot be accommodated within the AVR4-binding pocket as well as in avidin. Due to the proline residue (P41) in the L3,4 loop of AVR4, the loop also becomes somewhat “shorter” than the L3,4 loop in avidin. As a result, the mouth of the binding pocket of AVR4 is wider than in the avidin structure (Figure 2C). Since the *para*-derivatives of HABA are more elongated than the *ortho*- and *meta*-derivatives, they extend further out from the binding pocket. In avidin, the *para*-derivatives collide with T40, but, in AVR4, there is sufficient space to accommodate the longer *para*-derivatives (Figure 2C). These docking studies are in good agreement with our DSC studies, which show that AVR4 binds the *para*-compounds more strongly, while avidin has stronger binding affinity for the *ortho*-compounds.

The exception from the previous pattern is naphthyl-HABA, compound 3a, which, according to the DSC studies, has the highest affinity for both avidin and AVR4. According to the docking studies, avidin would bind this *ortho*-compound with the open conformation of the

L3,4 loop, in contrast to AVR4 with the added salt bridge that suggests binding might involve the closed loop conformation. The crystal structure of the streptavidin complex and compound 3a shows that 3a is bound to a closed loop conformation [26]. It seems that the shorter length of the L3,4 loop of streptavidin (Figure 2B) is the reason it adopts the closed loop conformation. Although the L3,4 loop of AVR4 also appears to be somewhat shorter than that of avidin (due to a kink in the loop introduced by P41), there are other features of the loop contributing to the mode of ligand binding. First of all, the salt bridge between the L3,4 loop and the β 8 strand holds the loop tightly in its position. Second, in the L3,4 loop of AVR4, the methyl group of A38 would form a hydrophobic interaction with the two-ring system of compound 3a. The corresponding residue in avidin is threonine (T38), which, due to its larger volume and polar hydroxyl group, hinders the binding of compound 3a to the closed L3,4 loop conformation of avidin.

Significance

The avidin family of biotin-binding proteins is widely exploited in biotechnological applications and, more recently, in nanobiotechnology. There are obvious advantages to using a high-affinity ligand that alters its spectral characteristics when bound to an avidin protein, allowing one to measure spectrophotometrically the degree of successful complexation that has occurred. The organic azo dye, HABA (4-hydroxyazobenzene-2-carboxylic acid), does undergo such spectral changes when the avidin-HABA complex is formed, but the binding affinity of avidin for HABA is much less than the extremely tight binding that occurs with biotin. Thus, in order for a HABA-type molecule to be of use, the affinity must be substantially improved or another avidin-like molecule with tighter binding for a HABA compound should be identified. Here, we synthesized 15 derivatives of HABA, and we analyzed their binding characteristics with avidin and with a related protein, AVR4, by using DSC and UV/visible spectroscopy. We show that a number of these derivatives do have higher affinity for avidin, but that some compounds prefer to bind to AVR4. To our knowledge, we have solved the first high-resolution 1.5 Å structure of avidin that reveals novel structural details about the L3,4 loop, a loop that appears to be a major determinant defining the binding preferences of avidin and AVR4 for the HABA compounds. Molecular modeling was used to help position the compounds within the ligand-binding sites in the 3D structures of avidin and AVR4. These studies reveal the molecular basis for differences in ligand binding and provide firm details that can be used to determine how to proceed with the protein structure-based approach used to modify azo compounds to achieve higher affinity and selectivity for avidin or AVR4.

Experimental Procedures

Chemicals

2-aminobenzoic acid, 2-nitrophenol, and 1,2-dihydroxybenzene were purchased from Fluka (Buchs, Switzerland), and 4-aminobenzoic acid, 2,6-dimethylphenol, and 1-naphthol were purchased from

Merck (Darmstadt, Germany). 1,2-dihydroxy-3-methylbenzene was purchased from Aldrich Chemical Company. 2-anilinonaphthalene-6-sulfonic acid (2,6-ANS) was from Invitrogen. D-biotin was purchased from Sigma, and chicken avidin was a generous gift from Belovo S.A., Bastogne, Belgium.

Synthesis and Characterization of Azo Molecules

HABA derivatives (for a table of the molecular structures, see Table 1) were synthesized by coupling diazotized aminobenzoic acid to the phenol and naphthol derivatives [26]. Ice-cooled aqueous NaNO₂ (7.3 mmol) was slowly poured into a stirred solution of *ortho*-/*meta*-/*para*-aminobenzoate (7.3 mmol) in hydrochloric acid (18%) while the temperature was kept below 5°C. The mixture containing the diazonium salt was cautiously poured into an ice-cooled aqueous solution of the phenol/naphthol derivatives (14.0 mmol) and NaOH (16.8 mmol). The reaction mixture was stirred at 5°C for 1 hr and neutralized with hydrochloric acid/sodium acetate. The resulting precipitates were collected, washed with water, and dried in vacuo. The product was recrystallized from the ethanol-water mixture and dried.

In the synthesis of 1,2-dihydroxyazobenzene carboxylic acid, 1,2,3-dihydroxyazobenzene carboxylic acid, and 1,2-dihydroxy-3-methylazobenzene carboxylic acid, the reactions were slightly different because the hydroxyl groups were protected by aluminum sulfate. Ice-cooled aqueous NaNO₂ (25 mmol) was poured into a stirred solution of *ortho*-/*meta*-/*para*-aminobenzoate (25 mmol) in hydrochloric acid (4.5%) while the temperature was kept below 5°C. 1,2-dihydroxybenzene/1,2,3-dihydroxybenzene/1,2-dihydroxy-3-methylbenzene (25 mmol) was diluted with aqueous Al₂(SO₄)₃ (14 mmol), and the diazonium salt solution was poured cautiously into this ice-cooled solution. The reaction mixture was stirred at 5°C for 40 min, and 25 ml CH₃COONa (20%) was added to the reaction mixture. The solution was acidified by adding 10 ml concentrated HCl, and the resulting reddish precipitates were collected, washed with water, and dried in vacuo. The products were recrystallized from an ethanol-water mixture and dried in vacuo.

The final products were confirmed by ¹H-NMR (Bruker Avance DPX 250 FT), ¹³C-NMR (Bruker Avance DPX 500), and by MS. The ¹H-NMR spectra were recorded at 250 MHz, and ¹³C spectra were recorded at 500 MHz in d-DMSO at 30°C. The detailed list of synthesized compounds with confirmed compound characteristics is in Supplemental Data.

Differential Scanning Calorimetry Analysis

The thermodynamics of the denaturation process of avidin isolated from chicken (Belovo S.A., Bastogne, Belgium) and the AVR4 protein produced in *E. coli* [14, 37], in the presence of different ligands (3:1 molar ratio), were studied by using a Nano II differential scanning calorimeter (Calorimetric Science Corporation, Provo, UT) as previously described [7]. AVR4 carried a mutation, C122S, that prevents intermolecular disulfide bridge formation without affecting either ligand binding or thermostability [16]. Sodium phosphate buffer (50 mM, pH 7.0) containing 100 mM NaCl was used in the measurements. Thermograms were analyzed with Origin 6.0 software. The apparent binding constant at the temperature of protein unfolding K_b(T_m) was calculated as described in Brandts et al. [32] by using the following equation:

$$K_b(T_m) = \left[\exp\left[-\frac{\Delta H(T_0)}{R(1/T_m - 1/T_0)} + \frac{\Delta C_p}{R(\ln T_m/T_0 + T_0/T_m - 1)}\right] - 1 \right] / [L]T_m \quad (1)$$

where $\Delta H(T_0)$ is the change in enthalpy upon unfolding in the absence of ligand, R is the gas constant, T_m is the unfolding temperature in the presence of ligand, T_0 is the unfolding temperature in the absence of ligand, ΔC_p is the change in heat capacity upon unfolding, and $[L]T_m$ is the free ligand concentration at T_m . It is assumed that the unfolding process is a two-state transition and that the ligands bind only to the low-temperature, native conformation. In the calculation of the binding constants, we used the respective values for avidin and AVR4: $\Delta H(T_0)$, 329 kJ/mol and 460 kJ/mol; ΔC_p , 15.3 kJ/(K mol) and 9.1 kJ/(K mol) [16]. The value of ΔC_p used for AVR4 originates from measurements performed on AVR4 protein produced in insect cells and not in bacteria. Even a significant deviation in the value of ΔC_p would, however, only have a very small

impact on the calculated K_b(T_m)s. Such a deviation would not affect the relative binding affinities for one protein and several different ligands.

UV/Visible Spectroscopy

The optical properties of the synthesized azo compounds were characterized with a PerkinElmer UV/visible spectrometer. Spectra were obtained for samples in 50 mM Na-phosphate buffer (pH 7.0) containing 100 mM NaCl. The azo compounds were diluted to a final concentration of 20 mM, and the spectrum for each compound was measured at wavelengths between 300 and 650 nm. Furthermore, the spectrum of each of the azo compounds (20 mM) in the presence of 1 mg/ml chicken avidin (Belovo S.A., Bastogne, Belgium) or AVR4 (produced in *E. coli* [14]) was measured. The spectrum for each compound was analyzed by using multipeak analysis (Microcal Origin 7.0), fitting two Gaussian peaks to the data.

Crystal Structure Determination

The recombinant chicken avidin protein used for structure determination with X-ray crystallography was produced in *E. coli*, purified, and crystallized as previously described [14]. Briefly, bar-like crystals were obtained at +22°C by using the hanging drop vapor diffusion method. Equal volumes (1 μ l) of protein (0.5 mg/ml) in 50 mM Na acetate (pH 4) + 20 mM NaCl and well solution of 0.1 M MES (pH 6.6) + 24% PEG 8000 + 0.2 M Mg acetate were employed. Before data collection, a crystal was soaked with compound 3a (1 mM in drop) for several hours at +22°C. Glycerol (23% v/v) was added to the crystallization drop to serve as a cryoprotectant just prior to flash freezing in a 100 K nitrogen stream.

Diffraction data were collected at 100 K at the synchrotron beamline X13 (EMBL-Hamburg) from a single crystal. The data were indexed, integrated, and scaled with the program package XDS [38]. The structure was solved with the molecular replacement technique and by applying programs from the CCP4i Suite [39]. An existing 2.7 Å avidin structure (PDB code 1AVD [31]) was used as a trial model in molecular replacement, which was carried out with the program AMoRe [40]. The X-ray structure was refined with Refmac5 [41] by using TLS [42] and was modified and rebuilt with the program O [43]. Solvent atoms were added to the model with the automatic procedure of ARP/wARP [44], whereas sulfate ions and glycerol molecules were added manually in O. The final model was analyzed with the programs PROCHECK [45] and WHATIF [46].

Docking Studies

The 3D structures of 2,6-ANS and the azo compounds (Table 1), including two different tautomers for each azo compound, were built and energy minimized in Sybyl (Tripos, St. Louis, MO). The Conjugate Gradient minimization method was used along with the MMFF94s force field and MMFF94 charges [47, 48]. The termination gradient was set to 0.05 kcal/mol, and the calculations were iterated until convergence was reached. The program GOLD 2.2 [49] was used for docking experiments, and all ligands, including both tautomers of the azo compounds, were docked. The standard default settings of GOLD were used, and the active site radius was set to 15 Å centered on the H_c atom of F79 of the avidin structure (PDB code 1VYO) and F81 of the AVR4 structure (PDB code 1Y55) [18]. The docking studies were performed based on the assumption that avidin binds the azo compounds in a manner similar to what has been observed for the avidin-HABA complex [20, 50]. In the docking studies, two distance constraints were used; otherwise, the program GOLD would not have managed to dock the azo compounds into the assumed conformation. The distance constraints were defined so that one of the carboxylate oxygens of the azo compounds was forced to be in the vicinity of the H_v atom of S16 and the H_n atom of Y33 (both in avidin and AVR4). The range of separation was from 1.5 Å to 3.5 Å, with a spring constant of 5.0.

Visualization

The Bodil modeling environment [51] was used for the visualization of the crystal structures as well as for the visualization of the docking results. Figures were produced with PyMOL version 0.99 [52], and labels were added by Gimp 2.2.

Supplemental Data

Supplemental Data include additional Experimental Procedures, which contain data on the isolation and characterization of the synthesized azo compounds, and are available at <http://www.chembiol.com/cgi/content/full/13/10/1029/DC1/>.

Acknowledgments

We thank the staff of beamline X13 at the European Molecular Biology Laboratory (EMBL)/DESY (German Synchrotron Research Centre) Hamburg for excellent support. This project was supported by the European Community—Access to Research Infrastructure Action of the Improving Human Potential Programme to the EMBL Hamburg Outstation, contract no. HPRI-CT-1999-00017. We thank the CSC—Scientific Computing Ltd., Espoo, Finland for providing us with access to the program GOLD. This work was supported by grants from the Academy of Finland, the Technology Development Center (TEKES) of Finland, Sigrid Jusélius Foundation, National Graduate School in Informational and Structural Biology (ISB), and the Foundation of Åbo Akademi University (Center of Excellence Program in Cell Stress).

Received: June 2, 2006

Revised: August 11, 2006

Accepted: August 14, 2006

Published: October 20, 2006

References

- Green, N.M. (1975). Avidin. *Adv. Protein Chem.* 29, 85–133.
- Green, N.M. (1990). Avidin and streptavidin. *Methods Enzymol.* 184, 51–67.
- Chilkoti, A., and Stayton, P.S. (1995). Molecular origins of the slow streptavidin-biotin dissociation kinetics. *J. Am. Chem. Soc.* 117, 10622–10628.
- Freitag, S., Chu, V., Penzotti, J., Klumb, L., To, R., Hyre, D., Trong, I., Lybrand, T., Stenkamp, R., and Stayton, P. (1999). A structural snapshot of an intermediate on the streptavidin-biotin dissociation pathway. *Proc. Natl. Acad. Sci. USA* 96, 8384–8389.
- Hyre, D.E., Le Trong, I., Freitag, S., Stenkamp, R.E., and Stayton, P.S. (2000). Ser45 plays an important role in managing both the equilibrium and transition state energetics of the streptavidin-biotin system. *Protein Sci.* 9, 878–885.
- Marttila, A., Airenne, K., Laitinen, O., Kulik, T., Bayer, E., Wilchek, M., and Kulomaa, M. (1998). Engineering of chicken avidin: a progressive series of reduced charge mutants. *FEBS Lett.* 441, 313–317.
- Nordlund, H.R., Laitinen, O.H., Uotila, S.T., Nyholm, T., Hytönen, V.P., Slotte, J.P., and Kulomaa, M.S. (2003). Enhancing the thermal stability of avidin. Introduction of disulfide bridges between subunit interfaces. *J. Biol. Chem.* 278, 2479–2483.
- Nordlund, H.R., Hytönen, V.P., Laitinen, O.H., Uotila, S.T., Niskanen, E.A., Savolainen, J., Porkka, E., and Kulomaa, M.S. (2003). Introduction of histidine residues into avidin subunit interfaces allows pH-dependent regulation of quaternary structure and biotin binding. *FEBS Lett.* 555, 449–454.
- Weber, P.C., Ohlendorf, D.H., Wendoloski, J.J., and Salemme, F.R. (1989). Structural origins of high-affinity biotin binding to streptavidin. *Science* 243, 85–88.
- Livnah, O., Bayer, E.A., Wilchek, M., and Sussman, J.L. (1993). Three-dimensional structures of avidin and the avidin-biotin complex. *Proc. Natl. Acad. Sci. USA* 90, 5076–5080.
- Hyre, D.E., Amon, L.M., Penzotti, J.E., Le Trong, I., Stenkamp, R.E., Lybrand, T.P., and Stayton, P.S. (2002). Early mechanistic events in biotin dissociation from streptavidin. *Nat. Struct. Biol.* 9, 582–585.
- Ahroth, M.K., Kola, E.H., Ewald, D., Masabanda, J., Sazanov, A., Fries, R., and Kulomaa, M.S. (2000). Characterization and chromosomal localization of the chicken avidin gene family. *Anim. Genet.* 31, 367–375.
- Niskanen, E.A., Hytönen, V.P., Grapputo, A., Nordlund, H.R., Kulomaa, M.S., and Laitinen, O.H. (2005). Chicken genome analysis reveals novel genes encoding biotin-binding proteins related to avidin family. *BMC Genomics* 6, 41.
- Hytönen, V.P., Laitinen, O.H., Airenne, T.T., Kidron, H., Meltola, N.J., Porkka, E., Hörhå, J., Paldanius, T., Määttä, J.A., Nordlund, H.R., et al. (2004). Efficient production of active chicken avidin using a bacterial signal peptide in *Escherichia coli*. *Biochem. J.* 384, 385–390.
- Laitinen, O.H., Hytönen, V.P., Ahroth, M.K., Pentikäinen, O.T., Gallagher, C., Nordlund, H.R., Ovod, V., Marttila, A.T., Porkka, E., Heino, S., et al. (2002). Chicken avidin-related proteins show altered biotin-binding and physico-chemical properties as compared with avidin. *Biochem. J.* 363, 609–617.
- Hytönen, V.P., Nyholm, T.K., Pentikäinen, O.T., Vaarno, J., Porkka, E.J., Nordlund, H.R., Johnson, M.S., Slotte, J.P., Laitinen, O.H., and Kulomaa, M.S. (2004). Chicken avidin-related protein 4/5 shows superior thermal stability when compared with avidin while retaining high affinity to biotin. *J. Biol. Chem.* 279, 9337–9343.
- Hytönen, V.P., Maatta, J.A., Kidron, H., Halling, K.K., Horha, J., Kulomaa, T., Nyholm, T.K., Johnson, M.S., Salminen, T.A., Kulomaa, M.S., et al. (2005). Avidin related protein 2 shows unique structural and functional features among the avidin protein family. *BMC Biotechnol.* 5, 28.
- Eisenberg-Domovich, Y., Hytönen, V.P., Wilchek, M., Bayer, E.A., Kulomaa, M.S., and Livnah, O. (2005). High-resolution crystal structure of an avidin-related protein: insight into high-affinity biotin binding and protein stability. *Acta Crystallogr. D Biol. Crystallogr.* 61, 528–538.
- Green, N.M. (1970). Spectrophotometric determination of avidin and streptavidin. *Methods Enzymol.* 18, 418–424.
- Livnah, O., Bayer, A., Wilchek, M., and Sussman, J.L. (1993). The structure of the complex between avidin and the dye, 2-(4'-hydroxyazobenzene) benzoic acid (HABA). *FEBS Lett.* 328, 165–168.
- Weber, P.C., Wendoloski, J.J., Pantoliano, M.W., and Salemme, F.R. (1992). Crystallographic and thermodynamic comparison of natural and synthetic ligands bound to streptavidin. *J. Am. Chem. Soc.* 114, 3197–3200.
- Gonzales, M., Argarana, C.E., and Fidelio, G.D. (1999). Extremely high thermal stability of streptavidin and avidin upon biotin binding. *Biomol. Eng.* 16, 67–72.
- Williams, D.H., Stephens, E., and Zhou, M. (2003). Ligand binding energy and catalytic efficiency from improved packing within receptors and enzymes. *J. Mol. Biol.* 329, 389–399.
- Pugliese, L., Malcovati, M., Coda, A., and Bolognesi, M. (1994). Crystal structure of apo-avidin from hen egg-white. *J. Mol. Biol.* 235, 42–46.
- Korndörfer, I.P., and Skerra, A. (2002). Improved affinity of engineered streptavidin for the Strep-tag II peptide is due to a fixed open conformation of the lid-like loop at the binding site. *Protein Sci.* 11, 883–893.
- Weber, P.C., Pantoliano, M.W., Simons, D.M., and Salemme, F.R. (1994). Structure-based design of synthetic azobenzene ligands for streptavidin. *J. Am. Chem. Soc.* 116, 2717–2724.
- Huberman, T., Eisenberg-Domovich, Y., Gitlin, G., Kulik, T., Bayer, E.A., Wilchek, M., and Livnah, O. (2001). Chicken avidin exhibits pseudo-catalytic properties. Biochemical, structural, and electrostatic consequences. *J. Biol. Chem.* 276, 32031–32039.
- Nardone, E., Rosano, C., Santambrogio, P., Curnis, F., Corti, A., Magni, F., Siccardi, A.G., Paganelli, G., Losso, R., Aprea, B., et al. (1998). Biochemical characterization and crystal structure of a recombinant hen avidin and its acidic mutant expressed in *Escherichia coli*. *Eur. J. Biochem.* 256, 453–460.
- Pazy, Y., Eisenberg-Domovich, Y., Laitinen, O.H., Kulomaa, M.S., Bayer, E.A., Wilchek, M., and Livnah, O. (2003). Dimer-tetramer transition between solution and crystalline states of streptavidin and avidin mutants. *J. Bacteriol.* 185, 4050–4056.
- Pazy, Y., Kulik, T., Bayer, E.A., Wilchek, M., and Livnah, O. (2002). Ligand exchange between proteins. Exchange of biotin and biotin derivatives between avidin and streptavidin. *J. Biol. Chem.* 277, 30892–30900.
- Pugliese, L., Coda, A., Malcovati, M., and Bolognesi, M. (1993). Three-dimensional structure of the tetragonal crystal form of egg-white avidin in its functional complex with biotin at 2.7 Å resolution. *J. Mol. Biol.* 231, 698–710.

32. Brandts, J.F., and Lin, L.N. (1990). Study of strong to ultratight protein interactions using differential scanning calorimetry. *Biochemistry* 29, 6927–6940.
33. Green, N.M. (1965). A spectrophotometric assay for avidin and biotin based on binding of dyes by avidin. *Biochem. J.* 94, 23C–24C.
34. Mock, D.M., Lankford, G., and Horowitz, P. (1988). A study of the interaction of avidin with 2-anilino-naphthalene-6-sulfonic acid as a probe of the biotin binding site. *Biochim. Biophys. Acta* 956, 23–29.
35. Pazy, Y., Raboy, B., Matto, M., Bayer, E.A., Wilchek, M., and Livnah, O. (2003). Structure-based rational design of streptavidin mutants with pseudo-catalytic activity. *J. Biol. Chem.* 278, 7131–7134.
36. Ellison, D., Hinton, J., Hubbard, S.J., and Beynon, R.J. (1995). Limited proteolysis of native proteins: the interaction between avidin and proteinase K. *Protein Sci.* 4, 1337–1345.
37. Hytönen, V.P., Määttä, J.A., Nyholm, T.K., Livnah, O., Eisenberg-Domovich, Y., Hyre, D., Nordlund, H.R., Hörhå, J., Niskanen, E.A., Paldanius, T., et al. (2005). Design and construction of highly stable, protease-resistant chimeric avidins. *J. Biol. Chem.* 280, 10228–10233.
38. Kabsch, W. (1993). Automatic processing of rotation diffraction data from crystals of initially unknown symmetry and cell constants. *J. Appl. Crystallogr.* 26, 795–800.
39. CCP4 (Collaborative Computational Project, Number 4) (1994). The CCP4 suite: programs for protein crystallography. *Acta Crystallogr. D Biol. Crystallogr.* 50, 760–763.
40. Navaza, J. (1994). AMoRe—an automated package for molecular replacement. *Acta Crystallogr. A* 50, 157–163.
41. Murshudov, G.N., Vagin, A.A., and Dodson, E.J. (1997). Refinement of macromolecular structures by the maximum-likelihood method. *Acta Crystallogr. D Biol. Crystallogr.* 53, 240–255.
42. Howlin, B., Butler, S.A., Moss, D.S., Harris, G.W., and Driessen, H.P.C. (1993). Tlsan—Tls parameter-analysis program for segmented anisotropic refinement of macromolecular structures. *J. Appl. Crystallogr.* 26, 622–624.
43. Jones, T.A., Zou, J.Y., Cowan, S.W., and Kjeldgaard. (1991). Improved methods for building protein models in electron density maps and the location of errors in these models. *Acta Crystallogr. A* 47, 110–119.
44. Lamzin, V.S., and Wilson, K.S. (1993). Automated refinement of protein models. *Acta Crystallogr. D Biol. Crystallogr.* 49, 129–147.
45. Laskowski, R.A., MacArthur, M.W., Moss, D.S., and Thornton, J.M. (1993). Procheck—a program to check the stereochemical quality of protein structures. *J. Appl. Crystallogr.* 26, 283–291.
46. Vriend, G. (1990). WHAT IF: a molecular modeling and drug design program. *J. Mol. Graph.* 8, 52–56, 29.
47. Halgren, T.A. (1990). Maximally diagonal force constants in dependent angle-bending coordinates. Implications for the design of empirical force fields. *J. Am. Chem. Soc.* 112, 4710–4723.
48. Halgren, T.A. (1999). MMFF VI. MMFF94s option for energy minimization studies. *J. Comput. Chem.* 20, 720–729.
49. Jones, G., Willett, P., Glen, R.C., Leach, A.R., and Taylor, R. (1997). Development and validation of a genetic algorithm for flexible docking. *J. Mol. Biol.* 267, 727–748.
50. Kuhn, B., and Kollman, P.A. (2000). Binding of a diverse set of ligands to avidin and streptavidin: an accurate quantitative prediction of their relative affinities by a combination of molecular mechanics and continuum solvent models. *J. Med. Chem.* 43, 3786–3791.
51. Lehtonen, J.V., Still, D.-J., Rantanen, V.-V., Ekholm, J., Björklund, D., Iftikhar, Z., Huhtala, M., Repo, S., Jussila, A., Jaakkola, J., et al. (2004). BODIL: a molecular modeling environment for structure-function analysis and drug design. *J. Comput. Aided Mol. Des.* 18, 401–419.
52. DeLano, W.L. (2002). The PyMOL Molecular Graphics System (<http://www.pymol.org>).
53. Berman, H.M., Westbrook, J., Feng, Z., Gilliland, G., Bhat, T.N., Weissig, H., Shindyalov, I.N., and Bourne, P.E. (2000). The Protein Data Bank. *Nucleic Acids Res.* 28, 235–242.
54. Barton, G.J. (1993). ALSCRIPT a tool to format multiple sequence alignments. *Protein Eng.* 6, 37–40.

Accession Numbers

Coordinates have been deposited in the Protein Data Bank [53] with accession code 1VYO.